PVP-Vol. 313-2, International Pressure Vessels and Piping
Codes and Standards: Volume 2 — Current Perspectives
ASME 1995

INTERPRETING ASME LIMITS AND PHILOSOPHY IN FEA OF PRESSURE VESSEL PARTS

Luciano M. Bezerra, Julio R. B. Cruz, Carlos A. J. Miranda, M. Mattar Neto
Comissão Nacional de Energia Nuclear - IPEN
São Paulo, SP, Brazil

ABSTRACT

In recent years there has been an effort to interpret finite element (FE) stress results on the light of the ASME B&PV rules and philosophy. Many task groups have issued guidelines on stress linearization and classifications. All those attempts have come up trying to cope modern FE techniques with the rules imposed by the ASME Code. This paper is an independent contribution to the Pressure Vessel Research Council (PVRC) groups which are studying the stress classification and the failure mechanism in a FE framework. This work tries to complement the interesting work by Hollinger and Hechmer presented in the PVP-94 in Minneapolis [1]. In that paper, the authors examined a typical support skirt and showed relations between the skirt collapse load obtained by finite element analysis and the loads allowed from the ASME stress limits. To complement such paper, in the present article, different skirt geometry configurations are analyzed. The configurations here investigated consist of similar support skirts but with different angles of attachments between cylinder and cone parts. It will be possible to observe the influence of the bending stress in the collapse load and its relation to the allowable loads inferred from the ASME limits. A pressure vessel with torispherical head under internal pressure is also examined. Using elastic and limit load FEA, the present paper determines the collapse loads of the configurations. It sets up the relations between these collapse loads, stress categories, and limits dictated by the ASME Code Subsection NB. On the light of NB rules and philosophy, this paper shows how different methods of stress assessment, classification, and limits may influence in the design of a pressure vessel.

INTRODUCTION

The computer technology and structural modeling and analysis have had an overwhelming advance. This situation is completely different from the sixties when the "design by analysis" was put in the B&PV Code. The impact of computer technology and Finite Element Analysis (FEA) in engineering judgment is a real fact specially in the nuclear industry. These two technologies are essential tools in the modern workplace and are spread out worldwide. However, before verifying the stress results from FEA, the B&PV designer must understand the principles of the applicable Code. But some concepts in the Code (in this paper ASME Code refers to Subsection NB) may lead the designer to unnecessary expenses or unexpected structural collapse. The immediate impacts of this are the higher generating cost that will affect the prospects for a return to the building of new NPP and a threat to human being and the environment. This is a good time for technological changes because today the emphasis in the nuclear industry is not in the design of new units. The temporary halt of the nuclear industry turned the emphasis from the design and construction of new plants to the reliability, life-time extension and maintenance of operating units. There are several changes to the Code that must be done before the nuclear industry picks steam again.

This work is a modest and independent contribution to PVRC working groups on the stress classification and the failure mechanism in a FE framework. It focuses some of the critical points of ASME Subsection NB that need more attention such as stress assessment and stress classification. The use of FEA, in the design of complex geometry component, offers to the stress analyst the opportunity to calculate elastic stress and also limit-loads. Using FE results and NB rules, it is then possible to obtain allowable loads. The designer may observe that these allowable loads may be quite different. With such discrepancy in hand the designer can question the safety philosophy behind the simple ASME rules which are grounded on simple beam theory. The unrest observed in the engineering community is partly because, in certain situations, allowable ASME loads based on usual elastic stress results may lead to non conservative project. Using FE elastic and plastic analyses, this paper shows non conservative situations when allowable loads, based in different stress assessment and stress classification, are compared. The engineering community should look at these problems with responsibility and concern. The authors call attention that the goal here is not to sentence that the Code rules are completely inadequate and useless. On the contrary, it is well known that since 1915 - when B&PV Code was first published out - an outstanding record for safety was produced. But there are critical problems that must be addressed. A survey of weak links in ASME can be found in [1,2]. The present paper shows that the stress analyst can be taken to designs with no safety margins. The unclear concepts of the Code must be removed with responsibility and the same traditional ASME safety philosophy to strengthen and adequate the utility of the Code to the new and wide spread computer technologies and numerical modeling of today.

THE PROBLEM

In this paper, the work cited in reference [1] is extended a little bit more. In [1], the authors selected a support skirt configuration with a 18° of attachment between cone-cylinder. An end-load of 1122*psi* was also applied on the bottom cross section of the support cylindrical part. The authors in [1] have assessed the stress in the juncture using hand calculations based on simple beam theory ($\sigma = F/A \pm Mc/I$) and also with the help of FEA. In addition, the end-load was incremented and an elastic plastic analysis was undertaken so that a lower bound limit load was determined. Taking the Code definition of limit-load analysis as the intended basis for design, some conclusions were inferred from [1]. The main conclusions are: 1) the general primary stress, calculated by beam theory, gave an allowable load within 10% margin with respect to the limit-load results, 2) the membrane and/or bending stress was related to collapse mode, 3) beam theory gave a more conservative end-load than the end-loads based on elastic FEA. Our contribution in the present paper is to analyze three support skirts and also a torispherical pressure vessel adopting the same strategy used in [1] and to observe the extension of such conclusions. The limit-loads of each configuration will also be determined and compared with the diversity of loads allowed by the Code when different stress classification approach is used. It will be possible to observe the influence of the support skirt attachment angle between cone-cylinder on the allowable loads. Such attachment is responsible for the bending stress. The influence of the bending stress classification on the failure mode will also be observed.

GEOMETRIC CONFIGURATIONS

We have adopted the same type of skirt analyzed in [1]. However, the three skirts here analyzed are assembled by putting together the cylinder to the cone with different attachment angles not only 18° as in [1]. At the end of the cylindrical part an axial load is applied. This end-load consists of an arbitrary axis symmetric stress of F = 1122*psi* acting on the inferior cross section of the cylinder. The material properties, corresponding to the SA533-Gr.B, are $E = 29.5\times10^6 psi$ and $\nu = 0.3$. From the ASME Appendices [5], the allowable stress (S_m) is 26,700*psi* and the yielding stress (S_y) is 40,000*psi*. The cylindrical part of the support skirts has an internal radius R_i = 48.64*in* and a thickness t = 2*in*. The cone part is attached to the cylindrical part making an angle α with respect to the central axis. α is responsible for the bending stress in the cone-cylinder juncture area. Different α angles are used so that the impact of diverse bending values on the limit loads is investigated. The FE meshes of the skirts are depicted in Figures 1. The cone upper part is completely fixed. This simulates a rigid foundation for the support skirt. In addition to this boundary condition, also the nodes at the inferior section of the cylindrical part - where the end-load is applied - are coupled to simulate zero rotation. Taking into account the geometric change cone-cylinder and the locally applied stress at the bottom of the cylinder, an attenuation length of $5\sqrt{Rt}$ is considered. A blend radius of 2t in the juncture notch cylinder-cone is also used. Thus stress singularity in the notch can be prevented. In addition to the support skirts a pressure vessel is also analyzed. Such a vessel has the same internal radius and thickness of the skirt cylinder but is under an arbitrary internal pressure p = 450*psi*. The material is also the same one used for the support skirts. The tangential internal radius of curvature between the knuckle region and the spherical (crown) segment is L_i = 90*in*. The internal radius of the knuckle is r_i = 6*in*. The transitional angle between cylinder and crown is ϕ = 60° with respect to the horizontal axis. The FE mesh of the vessel is shown in Figure 1.

ELASTIC & LIMIT ANALYSES

The geometric configurations previously described are analyzed using the FEM available in the general purpose ANSYS software program. The arbitrary end-load of 1122*psi* in the support skirts, and the pressure of 450*psi* inside the torispherical vessel causes only elastic stresses in the respective component. Figure 1 shows the FE

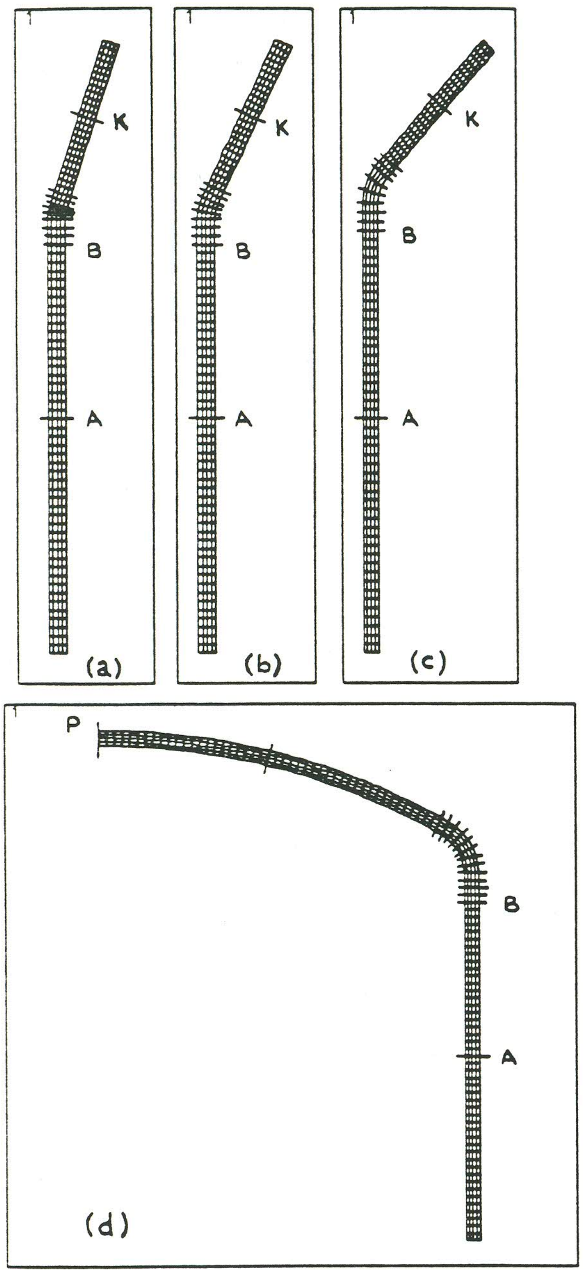

Figure-1 - (a) Skirt with $\alpha = 18°$, (b) Skirt with $\alpha = 25°$, (c) Skirt with $\alpha = 45°$, and (d) Pressure Vessel

models. Also in that figure, the stress classification lines "SCL," where the elastic stresses are linearized, are represented. Other than verifications with elastic analysis the ASME Code also admits the use of the plastic analysis. The limit analysis is a special case of plastic analysis taking the material as ideally plastic with no strain hardening. Considering a structure made of such material, a lower bound collapse load can be defined as the maximum load that such a structure can carry without an unbound increase of deformations.

In this paper, for the knowledge of the limit load of each configuration, the lower bound collapse approach is used. For the SA533-Gr.B, the collapse load can be achieved assuming that the stress-strain curve has an initial slope of $E = 29.5 \times 10^6 psi$, and a stress plateau at $S_y = 40.000 psi$. Accepting two-thirds of the lower bound collapse load is compatible with the ASME Code requirements to find the allowable load based on limit analysis. The classical bilinear option from ANSYS with the Von-Mises yield surface flow law was employed in the inelastic FE model. Very small load steps are adopted during the plastic analysis of the structures. For the skirts, an end-load increment of 100*psi* is applied whereas in the case of the torispherical vessel, pressure increments of 50*psi* are utilized. For the convergence criteria, the ANSYS default convergence criterion is put into action during the typical 10 iterations used for each load step increment. Tables-I to IV in the appendix summarize the results of the elastic FEA and Figure 2 shows the deformation of each structure on the onset of the collapse. The résumé presented in Table-A shows the collapse loads obtained for each configuration looked at in this study.

TABLE-A

Component Analyzed	Collapse Load
Skirt angle $\alpha = 18°$	36300 psi - end load
Skirt angle $\alpha = 25°$	30700 psi - end load
Skirt angle $\alpha = 45°$	18700 psi - end load
Pressure vessel	1200 psi - internal pressure

In Tables I, II, III, and IV, one can observe the regions with higher bending stresses. From Table-A, the high influence that the bending stress has on the final collapse load is clear.For the support skirts, it is straightforward the that the bigger the attachment angle α becomes, the smaller the collapse loads are. Thus, it should be reasonable to treat at least some share of the membrane + bending stress as primary stress [1]. The code considers, in areas of geometric discontinuity, membrane as local and bending as secondary.

STRESS ASSESSMENT & ALLOWABLE LOADS

The philosophy of "adequate safety" that is granted by the limits imposed to general primary membrane ($\leq S_y \div 1.5$) and primary membrane-plus-bending stress (S_y) in the ASME Code is based on the simple beam theory. In this paper, following the same steps presented in [1], the beam-approach collapse loads of the configurations here analyzed are set when the axial membrane stress, hypothetically, reaches the yielding stress value $S_y = 40{,}000 psi$. Considering the safety factor of 1.5, the allowable end-loads for all the skirt configurations are then obtained after dividing S_y per 1.5. The allowable

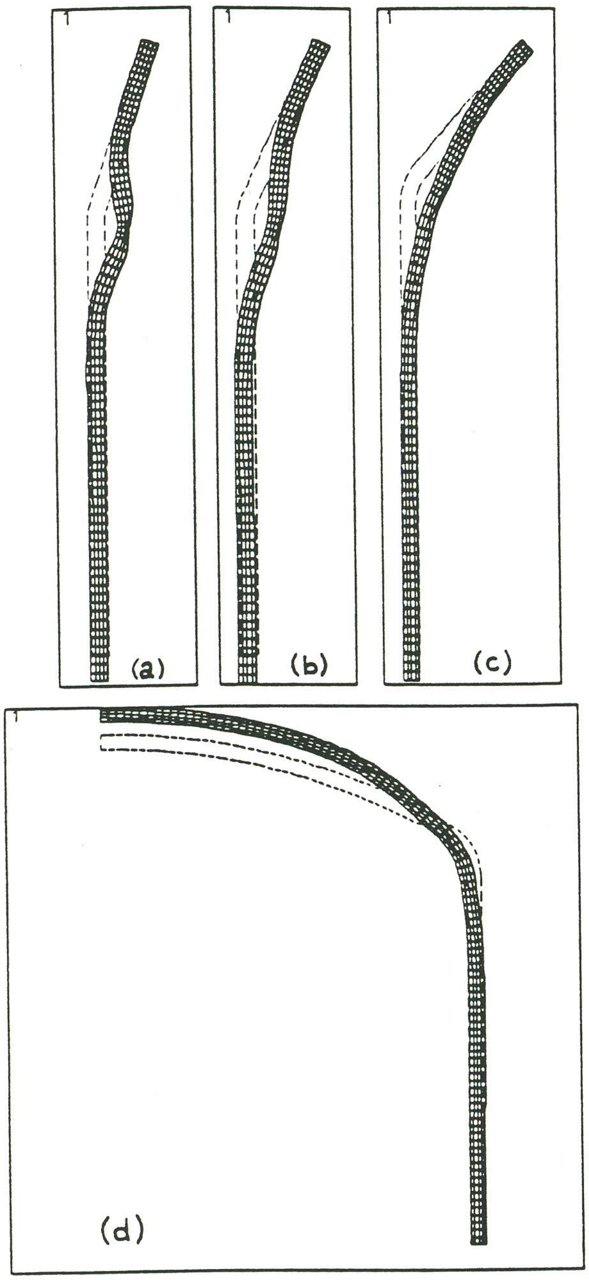

Figure-2 - Deformation on the onset of the collapse for the Skirt with (a) $\alpha = 18°$, (b) $\alpha = 25°$, (c) $\alpha = 45°$, and (d) Pressure Vessel

skirt end-load from the beam approach is then 26,700*psi*. For the vessel, the membrane stress in the cylinder is $\sigma = pR/t$ and in the spherical crown is $\sigma = pR/(2t)$. In the knuckle region the bending stress is predominant. Therefore, limiting the general membrane stress σ to 40,000*psi*, the maximum internal pressure can reach $t \times 40000 \div R$, or p = 1611*psi*. Applying the safety factor 1.5 for the general membrane stress, the allowable internal pressure is 1074*psi*.

Using the FE techniques one can establish a more precise value for the collapse load and, therefore, verify the robustness of the limits set by the ASME rules. Such approach was endeavored for the support skirt configurations and the pressure vessel described in the last paragraph. For the skirt with $\alpha = 18°$, the results reported hereon confirm the values given in [1]. For example, in the vicinity of the cylinder-cone juncture, the maximum membrane stress intensity is in SCL-J. The stress intensity there is dominated by the meridional stress and reaches 1153*psi*. It can be mentioned that our model is longer than the model of [1] and also because the nodes where the end-load was applied were coupled to zero the rotation of that cross section. In the bending region cylinder-cone, the membrane stress can be classified as a local stress (P_L). The Code rule limits local stress $P_L \leq 1.5S_m$ = 40,000*psi*. Thus, if the end-load of 1122 causes such a stress value, the maximum allowable end-load is then $40000 \times 1122 \div 1153$ = 38924*psi*. For the support skirt with $\alpha = 25°$, the maximum P_L stress intensity is reached at SCL-E and the value of P_L = 1562*psi*. In this case the maximum allowable end-load is $40000 \times 1122 \div 1562$ = 28732*psi*. Similarly, for the other skirt with $\alpha = 45°$ the maximum P_L is observed at SCL-E and gets to P_L = 3066*psi*. In such a case, the maximum allowable end-load, based on ASME local membrane limit, is $40000 \times 1122 \div 3066$ = 14637*psi*. For the pressure vessel, the maximum P_L stress intensity is reached at SCL-I and the value of P_L = 17130*psi* which gives an allowable internal pressure equal to $40000 \times 450 \div 17130$ = 1050*psi*.

Observing Table-I, II, and III, the maximum membrane + bending ($P_L + P_B$) stress intensities are achieved in SCL-F, SCL-F again, and SCL-G, respectively. The maxima ($P_L + P_B$) are: 2839*psi* in SCL-F for the skirt with $\alpha = 18°$, 3457*psi* in SCL-F for $\alpha = 25°$, and 5349*psi* in SCL-F for $\alpha = 45°$. For the pressure vessel, $P_L + P_B$ = 36980*psi*. Considering membrane + bending as primary stresses the Code limits $P_L + P_B \leq 1.5S_m$ = 40000*psi*. Taking such limiting value, the allowable end-loads for the skirts are: a) $40000 \times 1122 \div 2839$ = 15808*psi* for the skirt with $\alpha = 18°$, b) $40000 \times 1122 \div 3457 = 12982$*psi* for the skirt with $\alpha = 25°$, and c) $40000 \times 1122 \div 5349$ = 8390*psi* for the skirt with $\alpha = 45°$. For the vessel the allowable internal pressure is $40000 \times 450 \div 36980$*psi*. The ASME Code considers the bending stress in the cylinder-cone transition as secondary. Categorizing the membrane + bending as primary + secondary stress, the Code limits $P_L + P_B \leq 3S_m$ = 80000*psi*. Therefore, in such a case the allowable end-loads are the double of the values obtained before, i.e., 31616*psi*, 25964*psi*, and 16780*psi*, for the skirts with $\alpha = 18°$, 25°, and 45°, respectively. In the case of the pressure vessel, the allowable internal pressure is 972*psi*. It should be noted that if $P_L + P_B > 3S_m$ = 80000*psi* appropriate penalty factors should be applied for the fatigue evaluation, and also that appropriate verification should be performed to prevent ratcheting.

CONCLUSIONS

From Tables B, C, and D, it can be concluded that the simple beam theory, the elastic FEA, and the lower bound FE approaches gave extremely different results. It is obvious from the calculations that the stress classifications and the stress assessment methods influence the determination of the allowable loads. Taking the Code definition of Limit-Load Analysis as the basis for design, and comparing such allowable load with the other results, it can be concluded from Table B, C, and D that: (a) The beam approach gave greater allowable loads; (b) categorizing the membrane near structural discontinuity as PL also resulted in greater allowable loads; (c) taking membrane + bending near structural discontinuity as primary, produced smaller allowable loads; (d) considering membrane + bending at structural discontinuity as primary + secondary (P + Q) resulted in greater allowable loads. Notice that PM, PL, and PB limits are related to plastic collapse, while P + Q is related to fatigue and incremental plastic deformation.

The conclusions taken so far were grounded on the SCL's drawn in Figure 1. Those SCL's were selected on the basis of the designer's expertise. Before breaking up and classifying the stresses, it is wise to consider all the SCL's in conjunction with the Code recommendations [4] and also take into account the suggestions given in [2]. On the light of these recommendations and suggestions, some observations can be extracted.

TABLE-B

	End - Loads PSI - Cross Section					
	Cone at 18°		Cone at 25°		Cone at 45°	
	At Limit	Allowable	At Limit	Allowable	At Limit	Allowable
Beam - simple theory	40000	26700	40000	26700	40000	26700
FEA, M as PL	38924	38924	28732	28732	14637	14637
FEA, M + B as PL + PB	15808	15808	12982	12982	8390	8390
FEA, M + B as P + Q	31616	—	25964	—	16780	—
FEA, Limit Load	36300	24200	30700	20466	18700	12467

TABLE - C

		End-Load								
		Cone with18			Cone with 25			Cone with 45		
		At Limit	Allowable	SCL	At Limit	Allowable	SCL	At Limit	Allowable	SCL
Beam Theory		40000	26700	-----	40000	26700	-----	40000	26700	-----
FEA	M as PM	25648	25648	A	25238	25238	A	24043	24043	A
	M as PL	38924	38924	J	28732	28732	E	14637	14637	E
	M+B as PL+PB	15808	15808	F	12982	12982	F	8390	8390	G
FEA	M as PM	25648	25648	A	25238	25238	A	24043	24043	A
	M as PL	38924	38924	J	28732	28732	E	14637	14637	E
	M+B as P+Q	31616	-----	F	25964	-----	F	16780	-----	G
FEA, Limit Load		36300	24200	-----	30700	20466	-----	18700	12467	-----

TABLE - D

		Internal Pressure		
		At Limit	Allowable	SCL
Simple Theory	Cylinder	1611	1074	------
	Head	3223	2148	------
FEA	M as PM	1008	1008	A
	M as PL	1050	1050	I
	M+B as PL+PB	486	486	I
	M+B as PL+PB	1066	1066	O
FEA	M as PM	1008	1008	A
	M as PL	1050	1050	I
	M+B as P + Q	972	---	I
	M as PM	1066	1066	O
FEA, Limit Load		1200	800	-----

(a) For the skirt with α = 18°, see Table-B & C, the results confirm the observations and the conclusions given in [1]. However, we observe that in this case, both the beam theory and the elastic FEA results (away from the cone-cylinder juncture) approximate the plastic collapse end-load which is controlled by the higher stresses at the juncture. (b) For the skirt with α = 45°, see Tables B & C, the stress assessment based on elastic FEA (M as PL) shows an allowable load slightly greater than the FE limit-load analysis (14637*psi* against 12467*psi*). In this case, the allowable load based on the beam theory is much greater than the FE limit-load analysis (26700*psi* against 12467*psi*). The elastic FEA (at SCL-E) approximates the plastic collapse in the skirt much better than the simple beam theory. (c) For the skirt with α = 25°, see Tables B & C, neither the simple beam theory nor the elastic FEA gave allowable loads close to the FE limit-load analysis (26700*psi* and 25238*psi* against 20466*psi*). (d) For the pressure vessel, similar results are observed in Table-D. Categorizing membrane + bending as primary is too conservative but the simple hoop stress in the cylinder and the elastic FEA gave similar results, although greater (≈ 20-25%) than the FE limit-load analysis.

The pressure vessel case and the skirt with α = 25° case, among other cases, should be looked at with great care and responsibility. The results obtained may lead the stress analyst to non conservative designs putting in risk the environment or, elevating the costs. The engineering community urges that something sound has to be done so that these uncertaints can be carried off.

REFERENCES

[1]Hollinger , G. L. and Hechmer, J. L., 1993, "Three Dimensional Stress Evaluation Guidelines Progress Report," PVP-Vol. 277.

[2]Hollinger , G. L. and Hechmer, J. L., 1986, "Three Dimensional Stress Criteria - A Weak Link in Vessel Design and Analysis,"PVP-Vol. 109.

[3]ASME, 1968, "Criteria of the ASME Boiler and Pressure Vessel Code for Design by Analysis in Section III and VIII, Division 2, The American Society of Mechanical Engineering New York, NY.

[4]ASME, 1989, "Section III Rules for Construction of Nuclear Power Plant Components, Division 1 - Subsection NB, Class 1 Components." The American Society of Mechanical Eng., New York, NY.

[5]ASME, 1989, "Section III Rules for Construction of Nuclear Power Plant Components, Division 1-Appendices."The American Society of Mechanical Engineers, New York, NY.

[6]Hollinger , G. L. and Hechmer, J. L., 1991, "Three Dimensional Stress Criteria" PVP-Vol. 210-2

APPENDIX

TABLE - I: Support skirt with the attachment angle between cylinder and cone of $\alpha = 18°$ angle

SCL	TYPE	COMPONENTS				PRINCIPALS & SI			
—	——	RADIAL	LONG.	HOOP	SHEAR	S1	S2	S3	SI
A	M	-0.11	-1122	46.15	6.14	46.15	-0.07	-1122	1168
	$M+B_i$	-0.29	-1183	28.99	6.14	28.99	-0.26	-1183	1212
	$M+B_o$	0.28	-1061	63.31	6.14	63.31	0.32	-1061	1125
B	M	1.014	-1122	-937.7	-95.94	9.15	-937.7	-1130	1139
	$M+B_i$	6.55	-562.3	-794.2	-95.94	22.29	-578	-794.2	816.5
	$M+B_o$	-5.37	-1674	-1081	-95.94	0.12	-1081	-1680	1680
C	M	4.82	-1122	-1016	-115.6	16.57	-1016	-1134	1150
	$M+B_i$	8.15	-241.9	-779.1	-115.6	53.42	-287.2	-779.1	832.5
	$M+B_o$	-6.08	-1190	-1253	-115.6	0.63	-1253	-1997	1998
D	M	-3.86	-1122	-1083	-136.8	12.63	-1083	-1138	1151
	$M+B_i$	-4.28	139.4	-736.1	-136.8	222.1	-86.93	-736.1	958.2
	$M+B_o$	-5.43	-2367	-1430	-136.8	2.46	-1430	-2375	2377
E	M	-62.29	-1119	-1141	-157.4	-39.36	-1141	-1142	1103
	$M+B_i$	-27.77	499.6	-681.7	-157.4	543	-71.15	-681.7	1225
	$M+B_o$	-64.15	-2717	-1601	-157.4	-54.85	-1601	-2726	2671
F	M	-91.06	-1136	-1164	-52.50	-88.43	-1139	-1164	1076
	$M+B_i$	-32.17	682.5	-639.7	-52.50	686.3	-36.00	-638.7	1326
	$M+B_o$	-94.12	-2931	-1689	-52.50	-93.15	-1689	-2932	2839
G	M	-91.63	-1136	-1164	54.78	-88.77	-1139	-1164	1057
	$M+B_i$	-31.51	678.3	-637.2	54.78	682.5	-35.71	-637.2	1320
	$M+B_o$	-96.67	-2927	-1690	54.78	-95.61	-1690	-2928	2833
H	M	-64.24	-1119	-1140	159.6	-40.61	-1140	-1143	1102
	$M+B_i$	-27.11	514.2	-667.2	159.6	557.8	-70.68	-667.2	1225
	$M+B_o$	-64.15	-2732	-1613	159.6	-54.63	-1613	-2741	2686
I	M	-10.53	-1122	-1096	144.7	8	-1096	-1140	1148
	$M+B_i$	-6.22	215.8	-710.9	144.7	287.2	-77.57	-710.9	998.1
	$M+B_o$	-11.07	-2442	-1481	144.7	-2.49	-1481	-2451	2448
J	M	3.021	-1121	-1050	128.6	17.55	-1050	-1136	1153
	$M+B_i$	5	-98.60	-752.6	128.6	91.88	-185.5	-752.6	844.5
	$M+B_o$	-5	-2131	-1348	128.6	2.7	-1348	-2139	2142
K	M	-0.88	-1103	-448.6	11.83	-0.76	-448.6	-1103	1102
	$M+B_i$	1.96	-1601	-589.3	11.83	2.05	-589.3	-1601	1603
	$M+B_o$	-2.07	-610.6	-307.4	11.83	-1.84	-307.4	-610.8	609

TABLE - II: Support skirt with the attachment angle between cylinder and cone of 25° angle

SCL	TYPE	COMPONENTS				PRINCIPALS & SI			
—	—	RADIAL	LONG.	HOOP	SHEAR	S1	S2	S3	SI
A	M	-0.14	-1122	64.80	8.39	64.8	-0.08	-1122	1187
	$M+B_i$	-0.42	-1203	42.34	8.39	42.34	-0.36	-1203	1245
	$M+B_o$	0.4	-1042	87.25	8.39	87.25	0.46	-1042	1130
B	M	1.22	-1122	1300	-129.6	15.98	-1137	-1300	1316
	$M+B_i$	8.9	-427.3	-1125	-129.6	4.49	-462.9	-1125	1170
	$M+B_o$	-7.65	-1807	-1475	-129.6	1.62	-1475	-1875	1818
C	M	6.36	-1122	-1415	-156.9	27.79	-1143	-1415	1443
	$M+B_i$	11.69	6.58	-1114	-156.9	166.1	-147.8	-1114	1280
	$M+B_o$	-7.86	-2236	-1716	-156.9	3.14	-1716	-2247	2250
D	M	-6.63	-1122	-1517	-186.5	23.72	-1152	-1517	1540
	$M+B_i$	-6.99	525.7	-1066	-186.5	584.5	-65.79	-1066	1650
	$M+B_o$	-11.56	-2748	-1967	-186.5	1.08	-1967	-2760	2761
E	M	-88.92	-1117	-1608	-213.9	-46.21	-1160	-1608	1562
	$M+B_i$	-40.09	1038	-998.6	-213.9	1078	-80.98	-998.6	2077
	$M+B_o$	-91.29	-3243	-2218	-213.9	-76.84	-2218	-3258	3181
F	M	-143	-1150	-1657	-75.98	-137.3	-1156	-1657	1520
	$M+B_i$	-52.11	1324	-946.4	-75.98	1328	-56.29	-946.4	2274
	$M+B_o$	-138.3	-3592	-2368	-75.98	-136.6	-2368	-3594	3457
G	M	-144.2	-1152	-1654	67.83	-139.7	-1157	-1654	1514
	$M+B_i$	-51.28	1323	-933.5	67.83	1327	-54.62	-933.5	2260
	$M+B_o$	-143	-3597	-2375	67.83	-141.7	-2375	-3598	3456
H	M	-91.73	-1123	-1599	206.9	-51.75	-1163	-1599	1548
	$M+B_i$	-38.02	1072	-953.8	206.9	1109	-75.35	-953.8	2063
	$M+B_o$	-90.59	-3291	-2245	206.9	-77.27	-2245	-3305	3228
I	M	-14.61	-1129	-1527	187.5	16.09	-1160	-1527	1543
	$M+B_i$	-10.12	651.4	-1001	187.5	700.9	-59.59	-1001	1702
	$M+B_o$	-17.71	-2889	-2053	187.5	-5.51	-2053	-2901	2895
J	M	5.22	-1130	-1455	165.1	28.75	-1154	-1455	1484
	$M+B_i$	7.67	228.2	-1044	165.1	316.5	-80.61	-1044	1361
	$M+B_o$	-5.31	-2472	-1866	165.1	5.69	-1866	-2483	2489
K	M	-0.74	-1104	-575.2	6.31	-0.71	-575.2	-1104	1104
	$M+B_i$	2.48	-1764	-747.2	6.31	2.50	-747.2	-1764	1766
	$M+B_o$	-2.31	-452.4	-403.1	6.31	-2.22	-403.1	-452.5	450.3

TABLE - III: Support skirt with the attachment angle between cylinder and cone of 45° angle

SCL	TYPE	COMPONENTS				PRINCIPALS & SI			
—	—	RADIAL	LONG.	HOOP	SHEAR	S1	S2	S3	SI
A	M	-0.22	-1122	123.6	14.82	123.6	-0.02	-1122	1246
	$M+B_i$	-0.8	-1248	89.10	14.82	89.1	-0.62	-1248	1337
	$M+B_o$	0.76	-997.6	158.1	14.82	158.1	0.98	-997.8	1156
B	M	1.60	-1122	-2396	-221	43.51	-1164	-2396	2440
	$M+B_i$	15.20	-260.7	-2199	221	137.8	-383.3	-2199	2337
	$M+B_o$	-15.76	-1972	-2593	221	8.89	-1996	-2593	2602
C	M	8.55	-1122	-2643	-271.8	70.5	-1184	-2643	2713
	$M+B_i$	23.47	486	-2330	-271.8	611.6	-102.1	-2230	2841
	$M+B_o$	-10.25	-2709	-30.56	-271.8	16.85	-2736	-3056	3072
D	M	-27.12	-1122	-2875	-327.4	63.32	-1212	-2875	2938
	$M+B_i$	-28.06	1393	-2199	-327.4	1464	-99.88	-2199	3663
	$M+B_o$	-52.86	-3603	-3551	-327.4	-22.92	-3551	-3633	3610
E	M	-147.6	-1108	-3088	-369.1	-22.14	-1233	-3088	3066
	$M+B_i$	-34.83	2392	-2105	-369.1	2447	-89.73	-2105	4552
	$M+B_o$	-173.6	-4561	-4071	-369.1	-142.8	-4071	-4592	4450
F	M	-272.8	-1225	-3284	-161.3	-246.3	-1251	-3284	3038
	$M+B_i$	-68.69	3099	-2053	-161.3	3107	-76.88	-2053	5159
	$M+B_o$	-280.1	-5492	-4515	-161.3	-275.1	-4515	-5497	5222
G	M	-278.7	-1256	-3256	81.05	-272	-1262	-3256	2984
	$M+B_i$	-69.52	3178	-1938	81.05	3180	-71.54	-1938	5119
	$M+B_o$	-292.3	-5639	-4574	81.05	-291.1	-4574	-5640	5349
H	M	-148.7	-1195	-3031	317.4	-59.97	-1284	-3031	2971
	$M+B_i$	-19.11	2655	-1807	317.4	2692	-56.26	-1807	4500
	$M+B_o$	-162.4	-5011	-4255	317.4	-141.7	-4255	-5031	4890
I	M	-35.44	-1223	-2877	302.3	37.07	-1295	-2877	2914
	$M+B_i$	-39.56	1919	-1850	302.3	1965	-85.13	-1850	3815
	$M+B_o$	-56.78	-4337	-3904	302.3	-35.54	-3904	-4358	4322
J	M	3.15	-1239	-2727	270.3	59.41	-1295	-2727	2786
	$M+B_i$	12.77	1228	-1875	270.3	1286	-44.63	-1875	3161
	$M+B_o$	-5.45	-3684	-3579	270.3	14.31	-3579	-3704	3718
K	M	4.10	-1254	-2575	240.5	48.53	-1298	-2575	2624
	$M+B_i$	8.69	614	-1881	240.5	697.9	-75.26	-1881	2579
	$M+B_o$	-9.50	-3104	-3269	240.5	9.08	-3123	-3269	3279

TABLE - IV: Pressure vessel with torispherical head under internal pressure

SCL	TYPE	COMPONENTS				PRINCIPALS & SI			
—	—	RADIAL	LONG.	HOOP	SHEAR	S1	S2	S3	SI
A	M	-221.2	5362	11700	77.34	11700	5363	-222.3	11920
	$M+B_i$	-454.5	4901	11800	77.34	11800	4902	-455.7	12260
	$M+B_o$	5	5817	11590	77.34	11590	5818	3.97	11590
B	M	-224.3	5362	-2750	-1060	5556	-418.7	-2750	8306
	$M+B_i$	-362.8	5512	-2821	-1060	5697	-548.2	-2821	8518
	$M+B_o$	-88.79	5214	-2679	-1060	5418	-292.8	-2679	8097
C	M	-237.7	5362	-4553	-1354	5672	-548	-4553	10230
	$M+B_i$	-363.8	9176	-3578	-1354	9365	-552.2	-3578	12940
	$M+B_o$	-112	1598	-5529	-1354	2345	-858.4	-5529	7874
D	M	-146.3	5362	-6272	-1684	5836	-620.3	-6272	12110
	$M+B_i$	-279.6	13780	-3976	-1684	18980	-478.5	-3976	17950
	$M+B_o$	-16.86	-2944	-8567	-1684	750.6	-3711	-8567	9318
E	M	295.2	5293	-7770	-2022	6009	-420.1	-7770	13780
	$M+B_i$	88.33	19020	-3906	-2022	19230	-125.1	-3906	23140
	$M+B_o$	178.8	-8251	-11630	-2022	638.5	-8711	-11630	12270
F	M	706.6	5676	-8975	-1601	6147	235.7	-8975	15120
	$M+B_i$	421.1	24790	-3329	-1601	24890	316.4	-3329	28220
	$M+B_o$	249.8	-13180	-14620	-1601	437.9	-13370	-14620	15060
G	M	993	5958	-9904	-1138	6206	744.5	-9904	16110
	$M+B_i$	666.7	29430	-2921	-1138	29470	621.8	-2921	32390
	$M+B_o$	420.3	-17210	-16890	-1138	493.4	-16890	-17280	17780
H	M	1127	6223	-10470	-644.5	6303	1047	-10470	16770
	$M+B_i$	785.6	32600	-2704	-644.5	32620	772.5	-2704	35320
	$M+B_o$	468.7	-19840	-18230	-644.5	489.1	-18230	-19860	20340
I	M	1180	6676	-10410	493.4	6720	1137	-10410	17130
	$M+B_i$	810.5	34010	-2966	493.4	34020	803.1	-2966	36980
	$M+B_o$	528.1	-20380	-17850	493.4	539.7	-17850	-20390	20930
J	M	952.7	6833	-9985	1157	7052	733.2	-9985	17040
	$M+B_i$	595.6	31840	-3690	1157	31890	552.8	-3690	35580
	$M+B_o$	370.7	-17960	-16280	1157	443.5	-16280	-18030	18480
K	M	473.2	6838	-9532	1850	7337	-25.34	-9532	16870
	$M+B_i$	217.7	27760	-5002	1850	27880	93.98	-5002	32880
	$M+B_o$	279.3	-13930	-14060	1850	516.2	-14060	-14170	14680
L	M	-65.83	7189	-8913	1670	7555	-431.8	-8913	16470
	$M+B_i$	-241.4	23340	-6227	1670	23460	-359.1	-6227	29690
	$M+B_o$	80.2	-8847	-11600	1670	382.4	-9150	-11600	11980
M	M	-204.7	7489	-8021	1462	7757	-453.3	-8021	15780
	$M+B_i$	-350.3	19030	-7006	1462	19140	-460	-7006	26150
	$M+B_o$	82.2	-3972	-9036	1462	406.2	-4461	-9036	9442
N	M	-197.5	7786	-6957	1266	7981	-393.3	-6957	14940
	$M+B_i$	-347.6	15290	-7389	1266	15390	-449.4	-7389	22780
	$M+B_o$	-67.74	333.9	-6525	1266	1415	-1148	-6525	7940
O	M	-245.8	11020	10710	-214.6	11020	10710	-249.9	11270
	$M+B_i$	-432.6	6424	8667	-214.6	11010	6431	-439.3	9106
	$M+B_o$	-35.94	15580	12760	-214.6	15580	12760	-38.89	15620
P	M	-357.3	10960	10960	0	10960	10960	-357.3	11320
	$M+B_i$	-673.2	12060	12060	0	12060	12060	-673.2	12740
	$M+B_o$	-281.8	9859	9859	0	9859	9859	-281.8	10140